analytical chemistry

pubs.acs.org/ac

Technical Note

Surface-Enhanced Raman Spectroscopy-Scanning Electrochemical Microscopy: Observation of Real-Time Surface pH Perturbations

Kendrich O. Hatfield, Matthew T. Gole, Noah B. Schorr, Catherine J. Murphy, and Joaquín Rodríguez-López*

Cite This: *Anal. Chem.* 2021, 93, 7792–7796

Read Online

ACCESS | Metrics & More | Article Recommendations | Supporting Information

ABSTRACT: Understanding and controlling chemical dynamics at electrode interfaces is key to electrochemical applications in sensing, electrocatalysis, and energy storage. Here, we introduce colocalized surface-enhanced Raman scattering-scanning electrochemical microscopy (SERS-SECM) as a multimodal tool able to simultaneously probe and affect electrochemical interfaces in real time. As a model system to demonstrate SERS-SECM, we used a self-assembled monolayer of 4-mercaptopyridine (4MPy), a pH sensitive Raman indicator, anchored to silver nanoparticles as a substrate. We modulated the local pH at the surface with chronoamperometry, inducing the hydrogen evolution reaction (HER) at the SECM tip and observed subsequent Raman peak height changes in the 4MPy. We then performed cyclic voltammetry of HER at the SECM tip while measuring SERS spectra every 200 ms to highlight the technique's real-time capabilities. Our results show the capability to sensitively interrogate and trigger chemical/electrochemical dynamic surface phenomena. We hope SERS-SECM will provide insight on the link between heterogeneous and homogeneous reactivity at electrochemical interfaces.

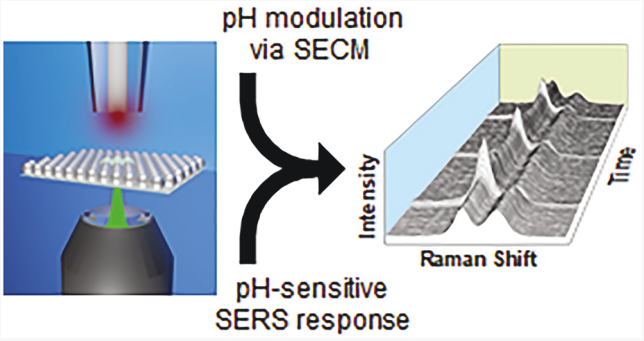

Controlling molecular surface dynamics at the electrode/electrolyte interface is critical to the advancement of energy storage, electrocatalysis, and electrochemical sensing. While electroanalytical techniques allow insight into the energetics and quantitation of electron transfer processes, alone, they are unable to unambiguously identify chemical structures and intermediates at an electrochemical interface. To compensate for this, much research is devoted to coupling electrochemistry with *in situ* and surface-sensitive vibrational spectroscopies.[1] Recent advancements in electrochemical surface- and tip-enhanced Raman spectroscopy[2,3] have yielded nanoscale spectroscopic data on electrochemical surfaces, yet the electrochemical responses measured are still that of the bulk sample. We recently reported on simultaneous, colocalized coupled Raman-scanning electrochemical microscopy (Raman-SECM), combining complementary features of these techniques in a real-time measurement platform.[4,5] Raman-SECM[4−7] enables spatially resolved probing of vibrational modes and *in situ* electrochemical reactivity. Unfortunately, Raman scattering is inherently weak, but enhancement is possible through several methods such as resonance Raman, where the excitation laser energy overlaps with that of an electronic transition of the sample. Previously, we have used resonance Raman with graphene[5] and polymeric materials[4] to sensitively probe surfaces with Raman-SECM. Here, we couple SECM with surface-enhanced Raman scattering (SERS) to sensitively control and detect processes confined to the interfacial region.

SERS increases Raman scattering by several orders of magnitude via interactions between the analyte and surface plasmons at a nanostructured surface[8] and is used extensively in electrochemical systems.[2] Researchers in the Schuhmann group devised a setup which could simultaneously image a substrate with SERS and SECM.[9] However, to our knowledge, no study to date has demonstrated simultaneous, colocalized SERS coupled with SECM (hereafter referred to as SERS-SECM) to monitor and/or trigger transient processes at interfaces. Others have coupled SECM to spectroscopic IR[10] and surface plasmon resonance methods[11] to understand the electrodeposition of bulk conducting polymers on a surface. The ability to interact with surface chemistries is a unique aspect of SECM that has enabled the identification of reactive adsorbed intermediates,[12] *in situ* growth[13] and modification of materials,[14,15] and read-write capabilities at surfaces;[16,17]

Received: February 26, 2021
Accepted: May 14, 2021
Published: May 27, 2021

https://doi.org/10.1021/acs.analchem.1c00888
Anal. Chem. 2021, 93, 7792−7796

simultaneously understanding these transformations would create exciting opportunities to judiciously explore and design functional interfaces. This work presents a proof-of-concept experiment demonstrating SERS-SECM as a tool to sensitively probe and perturb surfaces with temporal, lateral, and interfacial resolution.

We used pH-sensitive 4-mercaptopyridine (4MPy, Figure 1) covalently bonded to a monolayer of silver nanoparticles

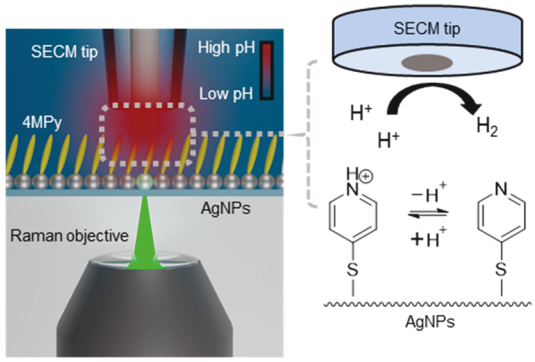

Figure 1. Surface chemistry and sensing strategy for SERS-SECM. The SECM tip alters local pH with HER above 4MPy anchored to silver nanoparticles, while a colocalized Raman objective collects SERS spectra to monitor the protonation state of 4MPy.

(AgNPs) deposited on glass as a substrate as a model system. 4MPy can assume neutral or cationic forms upon (de)-protonation and has pH-dependent spectral signatures.[18−21] The hydrogen evolution reaction (HER, eqs 1 and 2) at an electrode triggers a local pH change at the surface, and while its mechanism is pH-dependent, the effect is always to raise local pH either by consumption of protons or release of hydroxide ions.

$$\text{HER in acidic media:} \quad 2H^+ + 2e^- \rightarrow H_2 \tag{1}$$

$$\text{HER in basic media:} \quad 2H_2O + 2e^- \rightarrow H_2 + 2OH^- \tag{2}$$

Here, we use colocalized Raman-SECM, where the pH effects from HER at an SECM tip carry to the 4MPy decorated surface (Figure 1), and we distinctly identify these effects spectroscopically and correlate them to the electrochemical response. In addition to constant potential experiments, we perform cyclic voltammetry at the SECM tip while measuring SERS at specific time intervals. Ultimately, we successfully implement SERS-SECM to measure chemical changes at an interface with high sensitivity and high spatial and temporal resolution.

EXPERIMENTAL SECTION

Chemicals and Solution Preparation. Ferrocenemethanol (FcMeOH, 97%, Alfa Aesar), 4-mercaptopyridine (4MPy, 95%, Sigma-Aldrich), (3-aminopropyl)trimethoxysilane (APTMS, 97%, Sigma-Aldrich), silver nitrate ($AgNO_3$, 99%, Sigma-Aldrich), sodium citrate dihydrate ($Na_3C_6H_5O_7{\cdot}2H_2O$, Fisher Scientific), and citric acid (Fisher Chemicals) were purchased commercially and used as received. Methanol (99.9%, Fisher Chemicals) and ultrapure water from a Millipore Synergy purifier were used for all solutions. Potassium nitrate (KNO_3, 99%, Sigma-Aldrich) was used as the electrolyte. Nitric acid (HNO_3, Macron) and potassium hydroxide (KOH, 85%, Fisher Chemicals) were used alongside an Accumet model 15 pH probe to adjust the solution pH.

Silver Nanoparticle Synthesis. Colloidal silver nanoparticle synthesis was based on a citrate reduction method.[22] Briefly, 100 mL of H_2O and 18.0 mg of $AgNO_3$ were combined in a 125 mL Erlenmeyer flask and brought to a rolling boil while stirring at 600 rpm. A volume of 4 mL of 5% m/v sodium citrate dihydrate was added, and the reaction was stirred at a light boil for 60 min, during which the solution turned an opaque yellow-green color. The heat was then turned off and the solution cooled slowly while stirring on the hot plate for 60 min. The solution was centrifuged at 5000 relative centrifugal field for 15 min, after which the supernatant was discarded and the pellet diluted to 10 mL with nanopure water. This method yielded 65 ± 12 nm particles (TEM and size histogram in Figure S1a,b).

Substrate Fabrication. Glass coverslips were cleaned for 5 min in a Harrick-Plasma PDC-001-HP plasma cleaner (atmospheric air) on the highest energy setting before submerging the slides 30 min in 2% v/v APTMS in methanol. They were then rinsed with methanol before dropcasting AgNP solution onto them to cover the surface. The slides were left for 1 h before gentle rinsing with water. A transparent yellow coloring of the slide confirmed the presence of attached nanoparticles (Figure S1c). Enough 20 mM solution of 4-mercaptopyridine in methanol to cover the surface was dropcast onto the nanoparticle-coated coverslip and left to sit for 2 min before rinsing with methanol.

Instrumentation. A CH Instruments 920D SECM was used for all electrochemistry and positional control of the SECM tip and substrate. The Raman microscope used consists of a laser line (Melles Griot, 532 nm, 200 mW) passed through a neutral density filter bringing the laser power to 2 mW (unless otherwise noted) and focused onto the substrate from below through a 50× objective (Olympus; NA, 0.5). The backscattered photons were collected into a fiber optic cable connected to an Ocean Optics QE Pro spectrometer. For a detailed diagram, see Figure 1 in the work by Schorr et al.[5] Visualization of the SECM tip and laser spot at the substrate surface was obtained with an optical camera adapted to the microscope line.

SECM Tip Fabrication. The SECM tip was made by sealing a Pt wire (99.99% Purity, 25 μm diameter, Goodfellow) in one end of a glass capillary. The inside of the capillary was coated several times with conductive carbon paint thinned with isopropanol. Connection to an external wire at the other end was made with conductive silver epoxy. The tip was sharpened with sandpaper to a Rg of ∼3 and polished with 1 μm alumina gel.

Citrate Buffer Experimental Procedure. A 4MPy/AgNP coated coverslip was mounted into an SECM cell which was subsequently filled with an aqueous 0.1 M citric acid solution and pH adjusted by dropwise addition of dilute KOH. After the Raman microscope was focused onto the substrate, five SERS spectra were collected (5 s integration time for each spectrum), and the solution was exchanged for the next pH value (pH value was changed in increasing order from 2.48 to 12.80).

SERS-SECM Experimental Procedure. A 4MPy/AgNP coated coverslip was mounted into an SECM cell which was subsequently filled with an aqueous 10 mM KNO_3 solution adjusted to pH 2.81 with diluted HNO_3. The cell was mounted onto an $x-y$ stage connected to stepper motors. The SECM tip

https://doi.org/10.1021/acs.analchem.1c00888
Anal. Chem. 2021, 93, 7792−7796

approach was controlled with stepper motors. The cell was purged with argon gas (ultrahigh purity, Airgas) for 15 min before forming an argon blanket with the gas needle to exclude O_2 from the cell.

To approach the substrate, the SECM tip was held at −0.8 V to achieve steady-state HER current while lowering the tip. The Raman microscope lens was aligned to the tip with micropositioners. Spectra were collected with Ocean Optics software using 5 s of signal integration time (unless otherwise noted), providing spectra with a resolution of 5 cm^{-1}. After finishing the SERS-SECM experiment, the solution was replaced with dilute FcMeOH in 10 mM KNO_3 aqueous electrolyte, and approach curves were repeated using FcMeOH oxidation at the tip (0.5 V) to verify the tip's height above the substrate (approach curves included in Figure S2). A Pt wire acted as a counter electrode, and all potentials reported are vs a Ag/AgCl reference used in all SERC-SECM experiments.

Peak Fitting Procedure. Peak quantification at 1580 and 1620 cm^{-1} was performed with Python 3.2. The spectra backgrounds were estimated and subtracted with an iterative polynomial regression algorithm (PeakUtils module). Lorentz peaks were fitted with a nonlinear least-squares regression (SciPy module).

RESULTS AND DISCUSSION

4MPy is an established pH-sensitive Raman indicator[18−20] that readily forms a self-assembled monolayer (SAM) on plasmonic metals such as gold[19] and silver.[18,23] Here we use a 4MPy SAM on a monolayer of AgNPs anchored to a glass slide to demonstrate SERS-SECM. Figure 2a shows the spectral region of a 4MPy/AgNP sample with the most dramatic shifts in peak intensity immersed in citrate buffer solutions of varying pH.

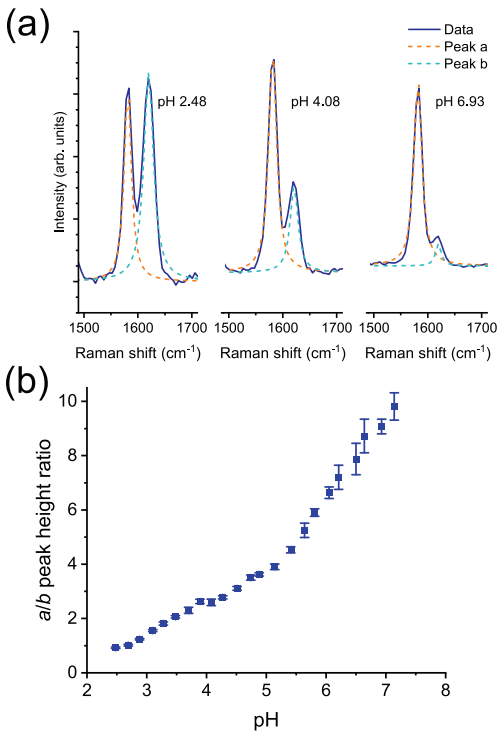

Figure 2. pH-dependent SERS spectra of 4MPy on AgNPs. (a) Example SERS spectra at select solution pH values. Lorentz fits for peaks a and b are shown with dashed lines. (b) Trend of the height ratio of peaks a and b versus pH.

The peaks at 1580 and 1620 cm^{-1} (from here on referred to as peaks a and b) are assigned to asymmetric and symmetric pyridine ring stretching, respectively.[23] Other peaks and their assignments are discussed in the Supporting Information alongside Figure S3. Figure 2a shows that peak a increases and peak b decreases while pH rises, agreeing with previous work.[18,19,21] To quantify this trend, we fit the peaks with Lorentz functions and plotted the a/b peak height ratio vs pH (Figure 2b), using this ratio to identify changes in surface pH. Yu et al. observed a spectral transition from pH 3−6, measuring a different set of peaks of 4MPy on a gold substrate,[19] attributing this to the change from cationic to neutral 4MPy. With the a and b peaks, we observe a similar transition from pH 3−4 as well as a more pronounced transition from pH 5−7. Hu et al. observed similar a and b peak trends to ours on silver,[18] and others have discussed the possibility of a further deprotonated anionic form of 4MPy, which could be responsible for this shift.[21]

For SERS-SECM, we used HER (eqs 1 and 2) at the SECM tip to perturb surface pH while measuring SERS with the colocalized Raman microscope, as depicted in Figure 1. Our setup is identical to that of our previous Raman-SECM studies,[4,5] with an SECM cell mounted on a stage with a Raman microscope objective below. By coaligning the tip with the objective, we can probe and interact with the substrate with spatial resolution dictated by the diameters of the laser spot (~3 μm) and tip (25 μm). We used a 10 mM KNO_3 solution adjusted to pH 2.81 and purged with argon to remove O_2.

After positioning the probe 10 μm above the substrate, we performed chronoamperometry and collected SERS spectra at the surface. As the tip is biased more negatively and current increases, the a/b peak height ratio rises (Figure 3). Figure S4 shows the a and b peaks at various tip potentials. The voltammogram in the Figure 3 inset (top) shows two processes associated with HER at the tip in bulk solution. These have been described previously for solutions at moderate pH values (including pH 3):[24] the first wave indicates electrolysis of H^+ and the second wave results from water electrolysis. The first process causes slight pH changes, causing an a/b ratio increase by 1.2−1.4× (Figure 3 inset, bottom). Water electrolysis induces a larger pH change, causing a/b ratio changes up to 8.4 at −1.4 V. This ratio is similar to those in the pH-controlled SERS experiments between pH 6 and 7 (Figure 2b). Recently, Monteiro et al. measured changes up to 3 pH units 75 μm away from a gold electrode performing HER.[25] Thus, the SERS-SECM observed pH changes from HER are reasonable.

After tip chronoamperometry, the a/b ratio measured with no pH modulation was 2.8 (Figure S5), higher than the initial ratio of 1.1. After ~5 min of laser exposure at our highest laser power (200 mW), the peak heights of a fresh sample stabilize. Thus, the changes observed over the course of SERS-SECM suggest a lasting effect of HER on the substrate. Zheng et al. observed similar peak height ratio changes that stabilize with time on 4MPy/Au surfaces exposed to a SERS laser.[26] They concluded that 4MPy moieties migrate about the imperfect surface, eventually bonding to the Au through both the S and N atoms, resulting in spectral shifts. We hypothesize that deprotonating 4MPy during SERS-SECM promotes similar behavior; pyridine is known to bind to silver surfaces through the N atom.[27]

To showcase the temporal resolution of SERS-SECM, we switched the neutral density filter to raise the power from 2 mW to 20 mW, allowing us to obtain clear spectra with an

https://doi.org/10.1021/acs.analchem.1c00888
Anal. Chem. 2021, 93, 7792−7796

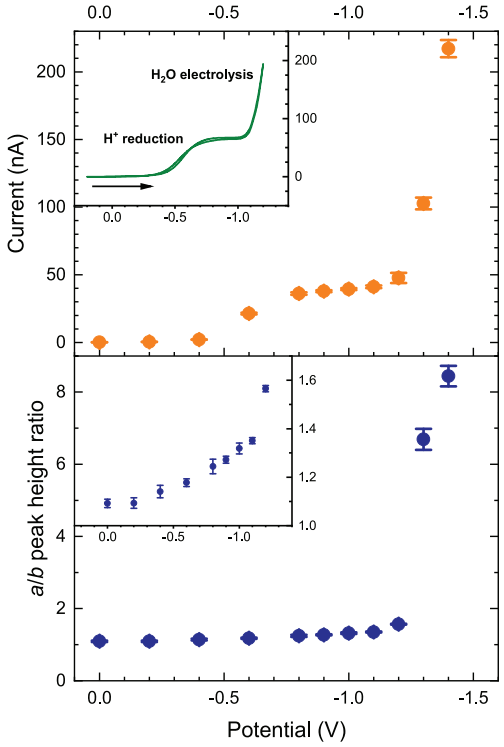

Figure 3. Chronoamperometric SERS-SECM experiment. (Top) Averaged tip current at different potentials (from 10 s onward); inset shows a voltammogram of HER at the tip in bulk solution (100 mV/s). (Bottom) Average a/b peak height ratio vs tip potential; inset shows a close view of ratios at potentials from 0 V to −1.2 V. Error bars indicate standard deviations of five measurements per potential value.

integration time of 200 ms. We performed a cyclic voltammogram at 100 mV/s 16 μm above a fresh substrate while measuring SERS (Figure 4). The a/b ratio begins at 1.4, spiking to 4.1 near −1.2 V alongside a tip current increase from water electrolysis. On the reverse sweep, the a/b ratio first rapidly decreased, followed by a gradual decrease to 1.8, higher than at the beginning of the voltammogram. Figure S6 shows the spectra of peaks a and b over the course of the voltammetric experiments. It must be kept in mind that plasmonic excitation can result in temperature jumps at the surface, with higher laser powers increasing this effect.[28] We repeated this cyclic voltammetric experiment at 5 mV/s with the OD 2 neutral density filter and 5 s integration and observed similar results (Figure S6). The choice of laser power for SERS-SECM should be tailored to the experiment to avoid degradation of analyte species and undesired substrate modification. Overall, this experiment demonstrates the ability of SERS-SECM to track localized dynamic surface changes over time.

CONCLUSIONS

We have shown dynamic SERS-SECM measurements via real-time SECM-probe induced pH changes to the Raman signal of an SAM of 4MPy adsorbed on AgNPs. Upon pH modulation, SERS spectra clearly detect the change in protonation state of the pyridine moieties. Further, we monitored these changes in real-time with SERS-SECM over the course of tip voltammetry. Interestingly, we found that reversible protonation is likely not the only change induced by electrochemical

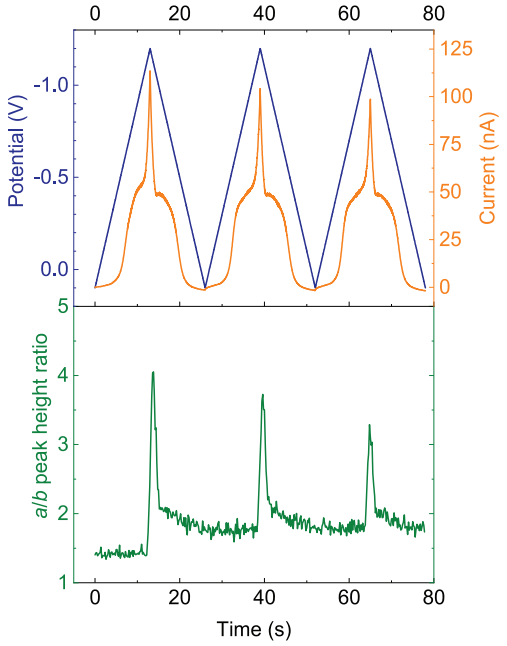

Figure 4. Voltammetric SERS-SECM experiment: (top) cyclic voltammogram displayed over time (blue, potential; orange, tip current); (bottom) a/b peak height ratio measured during the voltammogram. Scan rate, 100 mV/s; spectral integration time, 200 ms.

reactions at very negative potentials. SERS-SECM is a highly sensitive method ideal for examining spatiotemporally resolved chemical and electrochemical surface phenomena *in situ*.

ASSOCIATED CONTENT

Supporting Information

The Supporting Information is available free of charge at https://pubs.acs.org/doi/10.1021/acs.analchem.1c00888.

AgNP characterization, further peak assignments of 4MPy, approach curves, SERS spectra before, during, and after chronoamperometry, and SERS spectra during voltammetry (PDF)

AUTHOR INFORMATION

Corresponding Author

Joaquín Rodríguez-López − *Department of Chemistry, University of Illinois at Urbana−Champaign, Urbana, Illinois 61801, United States;* orcid.org/0000-0003-4346-4668; Phone: + 1-217-300-7354; Email: joaquinr@illinois.edu

Authors

Kendrich O. Hatfield − *Department of Chemistry, University of Illinois at Urbana−Champaign, Urbana, Illinois 61801, United States*

Matthew T. Gole − *Department of Chemistry, University of Illinois at Urbana−Champaign, Urbana, Illinois 61801, United States*

Noah B. Schorr − *Department of Chemistry, University of Illinois at Urbana−Champaign, Urbana, Illinois 61801, United States;* Present Address: N.B.S.: Department of Photovoltaics and Materials Technology, Sandia National Laboratories, Albuquerque, NM, 87185.; orcid.org/0000-0002-1582-8594

https://doi.org/10.1021/acs.analchem.1c00888
Anal. Chem. 2021, 93, 7792−7796

Catherine J. Murphy − *Department of Chemistry, University of Illinois at Urbana−Champaign, Urbana, Illinois 61801, United States;* orcid.org/0000-0001-7066-5575

Complete contact information is available at: https://pubs.acs.org/10.1021/acs.analchem.1c00888

Notes

The authors declare no competing financial interest.

■ ACKNOWLEDGMENTS

This material is based upon work supported by the National Science Foundation under CHE Grant 2004054 and the Illinois MRSEC, DMR Grant 1720633 and was carried out in part in the Materials Research Laboratory Central Research Facilities, University of Illinois.

■ REFERENCES

(1) Li, J. T.; Zhou, Z. Y.; Broadwell, I.; Sun, S. G. *Acc. Chem. Res.* **2012**, *45* (4), 485−494.
(2) Zaleski, S.; Wilson, A. J.; Mattei, M.; Chen, X.; Goubert, G.; Cardinal, M. F.; Willets, K. A.; Van Duyne, R. P. *Acc. Chem. Res.* **2016**, *49*, 2023−2030.
(3) Bao, Y. F.; Cao, M. F.; Wu, S. S.; Huang, T. X.; Zeng, Z. C.; Li, M. H.; Wang, X.; Ren, B. *Anal. Chem.* **2020**, *92*, 12548−12555.
(4) Gossage, Z. T.; Schorr, N. B.; Hernández-Burgos, K.; Hui, J.; Simpson, B. H.; Montoto, E. C.; Rodríguez-López, J. *Langmuir* **2017**, *33*, 9455−9463.
(5) Schorr, N. B.; Jiang, A. G.; Rodríguez-López, J. *Anal. Chem.* **2018**, *90*, 7848−7854.
(6) Steimecke, M.; Seiffarth, G.; Bron, M. *Anal. Chem.* **2017**, *89*, 10679−10686.
(7) Schorr, N. B.; Gossage, Z. T.; Rodríguez-López, J. *Curr. Opin. Electrochem.* **2018**, *8*, 89−95.
(8) Nie, S.; Emory, S. R. *Science* **1997**, *275* (5303), 1102−1106.
(9) Clausmeyer, J.; Nebel, M.; Grützke, S.; Kayran, Y. U.; Schuhmann, W. *ChemPlusChem* **2018**, *83*, 414−417.
(10) Wang, L.; Kowalik, J.; Mizaikoff, B.; Kranz, C. *Anal. Chem.* **2010**, *82* (8), 3139−3145.
(11) Szunerits, S.; Knorr, N.; Calemczuk, R.; Livache, T. *Langmuir* **2004**, *20* (21), 9236−9241.
(12) Counihan, M. J.; Setwipatanachai, W.; Rodríguez-López, J. *ChemElectroChem* **2019**, *6* (13), 3507−3515.
(13) Fedorov, R. G.; Mandler, D. *Phys. Chem. Chem. Phys.* **2013**, *15*, 2725−2732.
(14) Ktari, N.; Poncet, P.; Sénéchal, H.; Malaquin, L.; Kanoufi, F.; Combellas, C. *Langmuir* **2010**, *26* (22), 17348−17356.
(15) Zhang, M.; Su, B.; Cortés-Salazar, F.; Hojeij, M.; Girault, H. H. *Electrochem. Commun.* **2008**, *10* (5), 714−718.
(16) Wittstock, G.; Schuhmann, W. *Anal. Chem.* **1997**, *69* (24), 5059−5066.
(17) Noël, J. M.; Latus, A.; Lagrost, C.; Volanschi, E.; Hapiot, P. *J. Am. Chem. Soc.* **2012**, *134*, 2835−2841.
(18) Hu, J.; Zhao, B.; Xu, W.; Li, B.; Fan, Y. *Spectrochim. Acta, Part A* **2002**, *58*, 2827−2834.
(19) Yu, H. Z.; Xia, N.; Liu, Z. F. *Anal. Chem.* **1999**, *71*, 1354−1358.
(20) Jensen, R. A.; Sherin, J.; Emory, S. R. *Appl. Spectrosc.* **2007**, *61* (8), 832−838.
(21) Jung, H. S.; Kim, K.; Kim, M. S. *J. Mol. Struct.* **1997**, *407*, 139−147.
(22) Lee, P. C.; Meisel, D. *J. Phys. Chem.* **1982**, *86* (17), 3391−3395.
(23) Zhang, L.; Bai, Y.; Shang, Z.; Zhang, Y.; Mo, Y. *J. Raman Spectrosc.* **2007**, *38*, 1106−1111.
(24) Fernández, J. L.; Zoski, C. G. *J. Phys. Chem. C* **2018**, *122*, 71−82.
(25) Monteiro, M. C. O.; Jacobse, L.; Touzalin, T.; Koper, M. T. M. *Anal. Chem.* **2020**, *92*, 2237−2243.
(26) Zheng, X. S.; Hu, P.; Zhong, J. H.; Zong, C.; Wang, X.; Liu, B. J.; Ren, B. *J. Phys. Chem. C* **2014**, *118*, 3750−3757.
(27) Kaczor, A.; Malek, K.; Baranska, M. *J. Phys. Chem. C* **2010**, *114*, 3909−3917.
(28) Schorr, N. B.; Counihan, M. J.; Bhargava, R.; Rodríguez-López, J. *Anal. Chem.* **2020**, *92* (5), 3666−3673.